Using secondary tau neutrinos to probe heavy dark matter decays in Earth

Matthew Saveliev and Jeffrey Hyde*

Department of Physics & Astronomy, Bowdoin College, Brunswick, Maine 04011, USA

(Received 12 October 2021; accepted 18 April 2022; published 29 April 2022)

Dark matter particles can be gravitationally trapped by celestial bodies, motivating searches for localized annihilation or decay. If neutrinos are among the decay products, then IceCube and other neutrino observatories could detect them. We investigate this scenario for dark matter particles above $m_\chi \gtrsim$ PeV producing tau neutrino signals, using updated modeling of dark matter capture and thermalization. At these energies, tau neutrino regeneration is an important effect during propagation through Earth, allowing detection at distances far longer than one interaction length. We show how large energy loss of tau leptons above ∼PeV drives a wide range of initial energies to the same final energy spectrum of "secondary" tau neutrinos at the detector, and we provide an analytic approximation to the numerical results. This effect enables an experiment to constrain decays that occur at very high energies, and we examine the reach of the IceCube high-energy starting event sample in the parameter space of trapped dark matter annihilations and decays above PeV. We find that the parameter space probed by IceCube searches would require dark matter cross sections in tension with existing direct-detection bounds.

DOI: 10.1103/PhysRevD.105.083025

I. INTRODUCTION

Understanding the nature of dark matter is one of the most pressing issues in modern astrophysics, cosmology, and particle physics. Indirect detection of Standard Model particles produced in dark matter annihilations or decays is one way to gain an understanding of dark matter (DM) particles and how they may interact with familiar matter. Neutrino telescopes have the ability to detect and/or constrain neutrinos produced in this manner, especially decay of dark matter particles captured within the Sun or Earth [1–18]. So far, Super Kamiokande [19], AMANDA [20], and IceCube [21] have published limits on localized decay for dark matter particle masses around ~ 1–10^4 GeV.

Some work has considered decays of more massive particles [22–24], including as a possible explanation for the anomalous events seen by ANITA [25,26], and IceCube has also examined limits above 10^4 GeV [27]. However, recent work suggests that lower-energy secondary neutrinos would have been seen at IceCube, ruling out this explanation [11,28]. Models of heavy dark matter include decaying gravitinos [29] or right-handed neutrinos [30], while many of the above studies take a phenomenological approach that is agnostic to the particular model involved.

In this paper, we examine the current constraints and reach of IceCube in detecting high-energy neutrino decays from heavy dark matter particles trapped within the Earth, connecting IceCube event rates to dark matter properties, without restricting ourselves to the part of parameter space relevant to the ANITA events. We include a full treatment of tau neutrino propagation and regeneration [31–36] within the Earth, using a modification of NuTauSim [37], and give a semianalytic expression for the resulting spectra.

In particular, we examine the phenomenon of large tau lepton energy loss during propagation and emphasize the role it plays in setting constraints. Our work extends the pre-IceCube results of [7], and we use numerical and semianalytic calculations to provide a simple parametrization of the energy spectrum that will allow straightforward estimation of the effect of future observational developments on these constraints. Our work complements another recent paper [17]; in contrast with that work, we use a DM distribution localized very close to Earth's center based on the recent modeling of [38], we examine both decays and annihilations, and present constraints in terms of dark matter-nucleon cross sections and thermally averaged annihilation cross sections, to allow for comparison with specific dark matter models.

The structure of the paper is as follows. Section II describes the models and parameters that we investigate, and introduces the formalism that we use to describe the evolution of neutrino flux. Section III describes the simulation and presents our numerical and semianalytic results for high-energy neutrino propagation originating

*jhyde@bowdoin.edu

within the Earth. Section IV uses the results of Sec. III to examine the neutrino spectrum that would be seen at IceCube, as a function of the dark matter parameters. We use this to draw current constraints on the parameter space in comparison with direct detection bounds. Finally, in Sec. V we summarize our results, discuss implications and dependence on underlying assumptions, and consider possible extensions to future work.

II. MODELS AND PARAMETER SPACE

For greatest generality of our results, we consider two general scenarios that are commonly studied [13], and make minimal *a priori* assumptions about values of parameters or model-specific relationships between them. The general scenarios are as follows:

(1) Decay: examples include a heavy right-handed neutrino, ν_R, which can decay into a tau neutrino plus a Higgs [25,30], or a decaying gravitino [29]. We follow most studies in remaining agnostic to the particular model, considering the dark matter particle to have decay time τ_χ.
(2) Annihilation: dark matter particles annihilate via $X + X \to \nu + \nu$ (see review [13]), with thermally averaged cross section $\langle\sigma v\rangle$ a constant in v, i.e., s-wave annihilation.

We assume that there is either a direct decay to neutrinos (as in the above examples) or that any decay chain occurs quickly enough that we can reasonably approximate the neutrino source as the decay location. Our numerical results in Sec. III suggest that variations of $\lesssim$100 km do not significantly affect our conclusions. A longer-lived mediator would affect our results by reducing the number of neutrinos detected for given dark matter parameters, a point we return to in Sec. V.

Photons or charged leptons would generically accompany neutrino emission, but we do not consider potential observables related to these. We consider a spin-independent DM-nucleon cross section $\sigma_{\chi N}$ which scales as A^4, and in the case of decay, we take $m_\chi, \tau_\chi, \sigma_{\chi N}$ as independent free parameters, while for annihilation these are $m_\chi, \langle\sigma v\rangle, \sigma_{\chi N}$. We do not restrict ourselves to the assumption that dark matter was produced thermally in the early Universe, as nonthermal relics evade the unitarity bound that would otherwise preclude $m_\chi \gtrsim 10^5$ GeV [39].

We now describe the process of dark matter capture within Earth. First, we estimate annihilation and decay rates from the number density and distribution of dark matter particles within Earth. As Earth's galactic orbit passes through dark matter of density $\rho \simeq 0.3$ GeV/cm^3 at $v \approx 220$ km/s, particles fall into Earth's potential well and lose energy via collisions with nuclei, becoming trapped with $v < v_{\rm esc}$ (see [38] for a recent calculation). The captured particles thermalize on a timescale much shorter than the age of Earth, and settle into an equilibrium distribution which we represent in terms of the number density as

$$n(t,\vec{x}) = n_0(t)\exp(-r/r_0), \tag{1}$$

for constant r_0 and central number density $n_0(t)$. At any given time n_0 is normalized to the total number $N(t)$ of trapped particles. In particular, $N = \int d^3x n(t,\vec{x})$ gives $n_0 = N(t)/(8\pi r_0^3)$. Using $d\Gamma/dV = \langle\sigma v\rangle n(t,\vec{x})^2$, the annihilation rate is then [3,7,9]

$$\Gamma = \int d^3x \langle\sigma v\rangle n(t,\vec{x})^2 = \langle\sigma v\rangle N(t)^2/(64\pi r_0^3). \tag{2}$$

The number of captured particles may be approximated as [3]

$$N(t) = N_{\rm eq}\tanh(t/\tau), \tag{3}$$

where the eventual equilibrium number is $N_{\rm eq} = (C/C_A)^{1/2}$ and the timescale $\tau = (CC_A)^{-1/2}$, C is the capture rate, and $C_A \equiv \Gamma/N^2 = \langle\sigma v\rangle/(64\pi r_0^3)$ in our case. The age of Earth is significantly less than τ [9], so we can expand $\tanh(t/\tau) \approx (t/\tau)$, leading to $N(t) \simeq Ct$, so the annihilation rate is

$$\Gamma_{\rm ann.} \simeq \frac{\langle\sigma v\rangle C^2 t^2}{64\pi r_0^3}. \tag{4}$$

The extent r_0 of the thermalized dark matter distribution may be estimated as [38]

$$r_0 \simeq (2\text{ km})\left(\frac{10^7\text{ GeV}}{m_\chi}\right)^{1/2}, \tag{5}$$

when at Earth's core the temperature is 5000 K and density is 10 g/cm^3. We adopt these nominal values and therefore do not include slowly varying corrections that would account for different values. Furthermore, Ref. [38] estimates the capture rate for isotope-dependent (A^4) DM-nucleon scattering as

$$C_{\chi N} = \begin{cases} (2.45\times10^{22}\text{ s}^{-1})\left(\frac{10^3\text{ GeV}}{m_\chi}\right) & \text{for } \left(\frac{m_\chi}{1.66\times10^{12}\text{ GeV}}\right) < \left(\frac{\sigma_{\chi N}}{10^{-26}\text{ cm}^2}\right) \\ (8.74\times10^{27}\text{ s}^{-1})\left(\frac{10^8\text{ GeV}}{m_\chi}\right)^{7/2}\left(\frac{\sigma_{\chi N}}{10^{-26}\text{ cm}^2}\right)^{5/2} & \text{for } \left(\frac{m_\chi}{1.66\times10^{12}\text{ GeV}}\right) > \left(\frac{\sigma_{\chi N}}{10^{-26}\text{ cm}^2}\right) \end{cases}, \tag{6}$$

where capture is efficient for large enough cross section but drops rapidly below a certain value that depends on the mass. So, finally, we can combine Eq. (4) with Eqs. (5) and (6), including a factor of 2 to account for each annihilation producing two neutrinos, to find

$$\Gamma_{\rm ann} \simeq \begin{cases} (1.50\times10^{28}{\rm s}^{-1})(\frac{10^7\ {\rm GeV}}{m_\chi})^{1/2}(\frac{\langle\sigma v\rangle}{10^{-25}\ {\rm cm}^3{\rm s}^{-1}}) & \text{for } (\frac{m_\chi}{1.66\times10^{12}\ {\rm GeV}}) < (\frac{\sigma_{\chi N}}{10^{-26}\ {\rm cm}^2}) \\ (1.91\times10^{54}{\rm s}^{-1})(\frac{\langle\sigma v\rangle}{10^{-25}\ {\rm cm}^3{\rm s}^{-1}})(\frac{10^7\ {\rm GeV}}{m_\chi})^{11/2}(\frac{\sigma_{\chi N}}{10^{-26}\ {\rm cm}^2})^5 & \text{for } (\frac{m_\chi}{1.66\times10^{12}\ {\rm GeV}}) > (\frac{\sigma_{\chi N}}{10^{-26}\ {\rm cm}^2}) \end{cases}, \tag{7}$$

where we have used $t = 4.5$ Gyr as the age of the Earth. Our constraints in subsequent sections will take the DM-nucleon cross section $\sigma_{\chi N}$ and the thermally averaged DM self-annihilation cross section $\langle\sigma v\rangle$ to vary as independent parameters.

For the case of dark matter particles that decay with lifetime τ_χ, the decay rate is

$$\Gamma_{\rm decay} = \frac{1}{\tau_\chi}N(t) \simeq \frac{1}{\tau_\chi}Ct. \tag{8}$$

Again using capture rate estimate Eq. (6), we find

$$\Gamma_{\rm decay} \simeq \begin{cases} (2.45\times10^{22}\ {\rm s}^{-1})(\frac{10^3\ {\rm GeV}}{m_\chi})(\frac{t_{\rm Earth}}{\tau_\chi}) & \text{for } (\frac{m_\chi}{1.66\times10^{12}\ {\rm GeV}}) < (\frac{\sigma_{\chi N}}{10^{-26}\ {\rm cm}^2}) \\ (8.74\times10^{27}\ {\rm s}^{-1})(\frac{10^8\ {\rm GeV}}{m_\chi})^{7/2}(\frac{\sigma_{\chi N}}{10^{-26}\ {\rm cm}^2})^{5/2}(\frac{t_{\rm Earth}}{\tau_\chi}) & \text{for } (\frac{m_\chi}{1.66\times10^{12}\ {\rm GeV}}) > (\frac{\sigma_{\chi N}}{10^{-26}\ {\rm cm}^2}) \end{cases}. \tag{9}$$

We will take $\sigma_{\chi N}$ and τ_χ to be independent parameters in the analysis that follows.

Formally, we can express the neutrino flux arriving at a detector in terms of the observed energy E and the initial energy $\tilde{E}$ as

$$\frac{d\Phi}{dE} = 2\pi\int r^2 d\cos\theta\int d\tilde{E}\frac{d\Gamma}{dV}(r,\theta)f(E,\tilde{E},x)h(\tilde{E}), \tag{10}$$

where $d\Gamma/dV$ is the local decay or annihilation rate [defined by requiring $\Gamma = \int dV(d\Gamma/dV)$ with Eqs. (7) or (9)], r and θ are radial and polar coordinates in detector-centered spherical coordinates, and we have assumed azimuthal symmetry. The function $h(\tilde{E})$ gives the initial spectrum of decays, and $f(E,\tilde{E},x)$ is the probability for a neutrino of initial energy $\tilde{E}$ to arrive at the detector with energy E, traversing column depth $x \equiv \int dz\rho(z)$, where z is position along line of sight and $\rho(z)$ is local matter density. Due to the expected localization of heavy dark matter particles around Earth's center as in Eq. (5), we approximate all decays as occurring at the center, simplifying the above expression. The validity of this is further examined in Sec. III. We will see that the initial energy $\tilde{E}$ is irrelevant above $\sim10^7$ GeV, and therefore the form of $h(\tilde{E})$ will be irrelevant to most of our parameter space. In Sec. III, we numerically study evolution of neutrino flux through Earth in order to determine $f(E,\tilde{E})$.

III. PROPAGATION OF TAU NEUTRINOS WITHIN THE EARTH

As tau neutrinos propagate through the Earth, they undergo neutral current and charged current (CC) interactions with the surrounding rock. CC interactions occur approximately 72% of the time, and result in a shower of particles, including a tau lepton, which keeps some of the neutrino's energy. As it moves, the tau loses energy due to the photonuclear, Bremsstrahlung, and pair production effects (the first of which dominates at energies above $\sim10^8$ GeV), as a function of its current energy and the density of its surroundings. The particle eventually decays back into a tau neutrino, a stochastic event which occurs after the particle travels a randomized multiple of the tau decay length; this is tau neutrino regeneration [31–36]. We approximate the energy loss resulting from both the production and the decay of the τ as 30%. Before analyzing our numerical results, we discuss the energy loss of the tau leptons analytically to better illustrate certain features of the full results.

A. Semianalytic estimates

Since the photonuclear effect accounts for most energy loss above $\sim10^8$ GeV, we can describe the energy loss rate of a tau lepton of energy E as

$$\left\langle\frac{dE}{dx}\right\rangle \simeq -\beta(E)E, \tag{11}$$

where β is parametrized by

$$\beta(E) = p_0 + p_1(E/\mathrm{GeV})^{p_2}, \tag{12}$$

with $p_0 = 2.06 \times 10^{-7}$ cm^2 g, $p_1 = 4.93 \times 10^{-9}$ cm^2 g, $p_2 = 0.228$ in the ALLM parametrization [37,40]. The exponent causes β to vary slowly with energy, and in this section we approximate it by its value at $E = 10^8$ GeV, i.e., we take $\beta \simeq 5.0 \times 10^{-7}$ cm^2/g. Note that our numerical results use the full energy dependence. Integrating Eq. (11) under this approximation, we find

$$E = E_i e^{-\beta\rho z}, \tag{13}$$

where ρ is the average density along the tau's path, z is the distance travelled by the particle, and E_i is the initial energy of the tau lepton. Since the total energy loss depends on the distance traveled, which depends on the particle's lifetime and velocity, the distance is also dependent on the particle's energy. As an approximation, we assume the tau decays after exactly one lifetime (τ, or τ_0 in its rest frame), and express this as

$$1 = \int_0^{t_{\mathrm{dec}}} \frac{1}{\tau} dt = \int_0^{z_{\mathrm{dec}}} \frac{mc^2}{E} \frac{1}{c\tau_0} dz, \tag{14}$$

where m is the tau mass and z_{dec} represents the distance traveled during the tau's lifetime. Using Eq. (13) for the energy, evaluating the z integral and solving for the distance gives

$$z_{\mathrm{dec}} = \frac{1}{\beta\rho} \ln\left(\frac{\beta\rho c t_0 E_0}{mc^2} + 1\right). \tag{15}$$

This result can be used with Eq. (13) to show the tau's energy just before it decays, across a range of starting energies [as seen in Fig. 1(a)]; this shows that tau leptons above $\sim 10^8$ GeV lose energy until reaching approximately $10^{7.8}$ GeV, regardless of their starting energy. Above $\sim 10^8$ GeV the effect is dramatic, but approaching and below that point the energy losses become negligible. This can also be seen in Fig. 1(b): no matter their starting energy, the particles slow down dramatically within a short distance (relative to the path length of the tau lepton and neutrino) until reaching $\sim 10^{7.8}$ GeV, after which point they lose insignificant amounts of energy until decaying.

The stochastic nature of real decays means that the full numerical simulation in Sec. III B will find a distribution extending above and below a central value. Furthermore, the estimate of this section only considers propagation of a tau during one lifetime; the results of Sec. III B also account for energy losses during decays and more than one instance of tau propagation along the path, so they result in typical energies at the surface being lower. However, the phenomenon shown here—where high-energy tau propagation drives widely varying initial energies toward similar final energies—does carry over.

B. Numerical results

To produce an expected distribution of tau neutrino energies at the surface of the Earth, we use a modification of NuTauSim [37]. The Earth's density profile is modeled using the preliminary earth reference model [41]. Since the dark matter is localized around the center of the Earth [Eq. (5)] we approximate it to the exact center. That this is accurate can be seen in Fig. 2(a). Most of the dark matter is located well within 100 km of the center, and a 100 km displacement has a negligible effect on the propagation. Only at extreme distances, where effectively no neutrinos

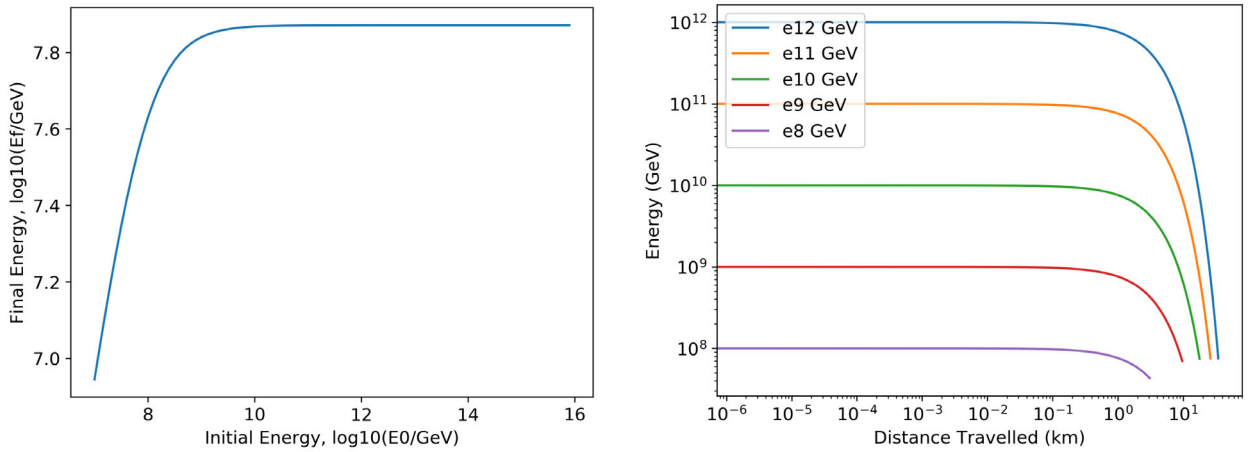

(a) (b)

FIG. 1. (a) The final energy of a tau lepton at the moment of decay as a function of its initial energy, using estimates Eqs. (13) and (15). (b) Tau lepton energies as they move through rock, for starting values between 10^8 and 10^{12} GeV. They travel exactly one lifetime, all decaying with energy $\sim 10^8$ GeV having traveled $\mathcal{O}(10^1$ km).

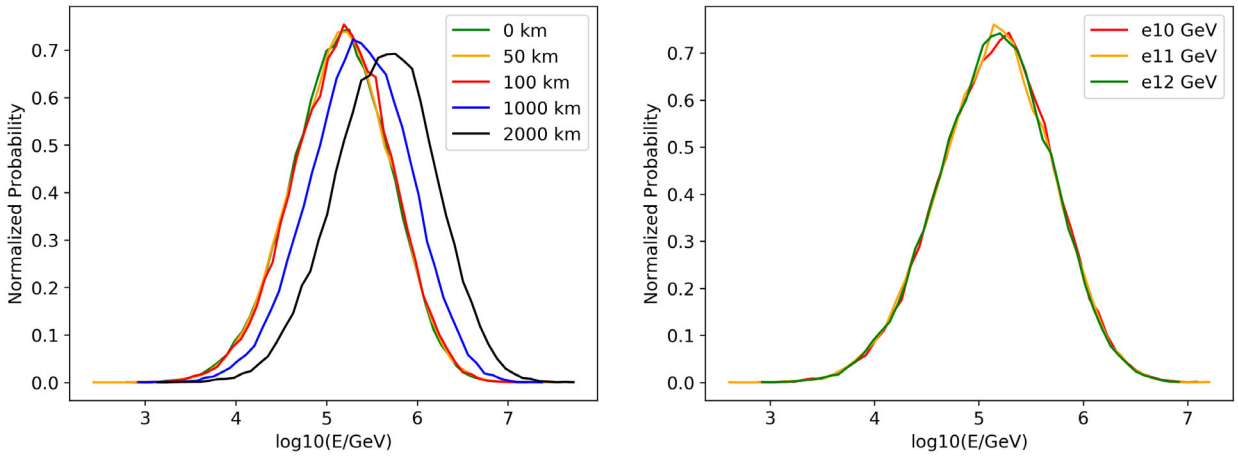

(a) (b)

FIG. 2. Panel (a) shows the final energy distribution of 10^{12} GeV neutrinos generated some distance from the center, along the line of sight. Panel (b) shows the final distribution of tau neutrinos generated at three different energies. Due to the effects in Fig. 1(b), the means and standard deviations of every distribution are within 5% of each other for energies between 10^7 and 10^{17} GeV.

are produced, does the displacement matter, so this is a good approximation.

The energy losses result in final energies at the Earth's surface being, on average, around 10^5 GeV, for all starting energies above $\sim 10^8$ GeV. This can be seen in Fig. 2(b), where each $f(E, \tilde{E})$ is given as a normalized probability density function (PDF) representing an average over ~50, 000 neutrinos numerically propagated from the center of the Earth. Since these distributions are nearly identical (for energies as high as 10^{17} GeV), they can be described with the following normalized probability distribution in terms of $\epsilon \equiv \log_{10}(E/\text{GeV})$:

$$f(\epsilon) = \frac{1}{\sigma\sqrt{2\pi}} e^{-\frac{1}{2}\left(\frac{\mu-\epsilon}{\sigma}\right)^2}, \tag{16}$$

where $\sigma = 0.541$ and $\mu = 5.148$.[1]

Below initial energies of 10^8 GeV, this becomes less accurate. The energy losses from the tau propagation stages become negligible next to those of neutral current and CC interactions, as well as the decay process of the tau leptons into tau neutrinos. As a result, neutrinos tend towards specific energies that depend on the number of interactions they experience, which can be seen in Fig. 3(a). The Gaussian gives way to several specific energy levels, an effect that becomes even more pronounced in Fig. 3(b). At 10^5 and 10^6 GeV, most neutrinos reach the surface with one of two energies: they either never interact and keep their initial energy, or undergo exactly one CC interaction and reach the surface with about 10% of their initial energy.

[1]So $f(E) = [\sqrt{2\pi}\sigma \ln(10)E]^{-1} \exp[(\log_{10}(E/\text{GeV}) - \mu)^2/(2\sigma^2)]$ is the normalized PDF in terms of E; this will be convenient in Sec. IV.

IV. PARAMETER REACH OF ICECUBE HESE EVENTS

As mentioned previously, we expect the general phenomenon described in Sec. III to be important for any observation of ultrahigh energy tau neutrinos. We now illustrate this effect by taking as an example the existing IceCube data set for high-energy starting events (HESE) at energies above 60 TeV over 2635 days of live time [42,43]. To date, the HESE sample consists of 60 events including two double cascade events that have been identified as tau neutrinos. This sample is consistent with a diffuse background with power-law energy dependence. For our analysis we exclude any region of parameter space that predicts 10 IceCube HESE events over 2635 days for energies greater than 60 TeV. We chose this as an estimate of a number of events that would be clearly localized compared with the 60 total events, and any $\mathcal{O}(10)$ number leads to essentially the same results. We also estimate the IceCube-Gen2 sensitivity following [44].

Formally, the number of events observed at IceCube during time T is

$$N = T \int dE \int d\tilde{E} f(E, \tilde{E}) \frac{d\Gamma}{d\tilde{E}} \frac{1}{4\pi R_\oplus^2} A_{\text{eff}}(E), \tag{17}$$

where (as before) E is the neutrino energy at the detector and $\tilde{E}$ is the energy at production (time of decay), and A_{eff} is the IceCube detector effective area for tau neutrinos (see e.g., [45]). For simplicity we approximate the decay spectrum of the dark matter particle with a delta function at 0.1 $m_\chi c^2$, although recalling the discussion of Sec. III A, the results will be almost independent of assumptions about this spectrum. We describe propagation using the results of Sec. III as encoded in Eq. (16), which leaves us with

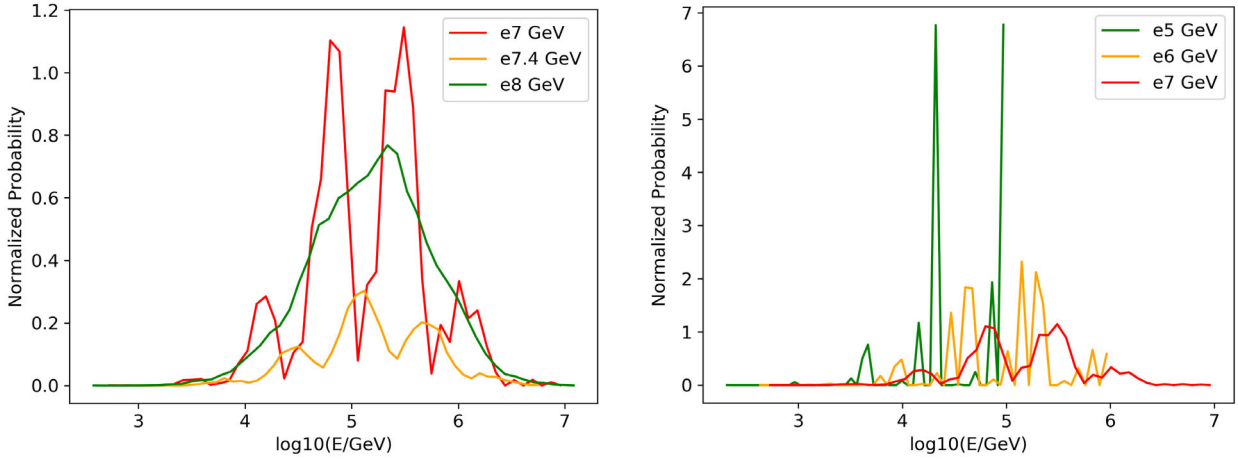

(a) (b)

FIG. 3. Normalized final energy distributions for neutrinos with initial energies between 10^7 and 10^8 GeV (a) and below 10^7 GeV (b)

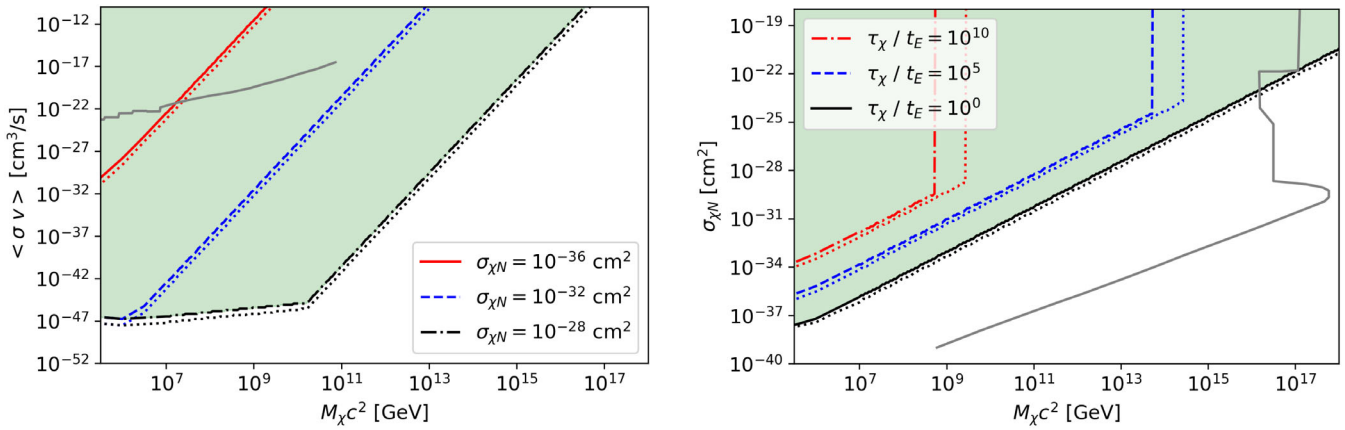

(a) (b)

FIG. 4. Parameter space reach of IceCube HESE events (dotted lines: IceCube-Gen2) for dark matter self-annihilation (a) and decay (b), for spin-independent (A^4-scaling) DM-nucleon cross sections. The gray line in (a) represents existing constraints on $\langle\sigma v\rangle$ [13]; the gray line in (b) shows $\sigma_{\chi N}$ constraints from [46]. In (b) the DM decay time is given as $\tau_\chi/t_{\rm E}$, where $t_{\rm E} = 4.5 \times 10^9$ years is the age of Earth. In (a) we see that the $\sigma_{\chi N}$ values needed to evade the bound we have computed for a given annihilation cross section are in tension with existing constraints on $\sigma_{\chi N}$ [compare with solid gray line in (b)].

$$N = T\frac{\Gamma}{4\pi R_\oplus^2}\int_{60\ \mathrm{TeV}}^{\infty} dE f(E,\tilde{E}) A_{\rm eff}(E). \qquad (18)$$

We use Eqs. (7) or (9) for annihilation or decay rates, use the IceCube effective areas for tau neutrino detection [42,45], and evaluate the integral Eq. (18) numerically using the results of Sec. III. Sampling the parameter space of m_χ, σ we find constrained regions shown in Fig. 4. Figure 4(a) shows the case of dark matter self-annihilation, while Fig. 4(b) shows the case of dark matter decay. In both cases, projected IceCube-Gen2 limits are included as dotted lines. Note that despite the formal upper limit on the integral in Eq. (18), the Gaussian tail from Eq. (16) causes the integrand to rapidly drop by 10^7 GeV, so the result is fairly insensitive to details of IceCube's highest energy reach.

For decays above $\sim 10^7$ GeV, the variation of the constraint curve with mass is entirely due to the annihilation rate, Eq. (7), or decay rate, Eq. (9). This is clear in Eq. (18), where the form of $f(E,\tilde{E})$ in Eq. (16) causes the integral to have no dependence on the initial energy or mass scale. This effect makes the features of the plot above

$\sim 10^7$ GeV easy to understand. First, we use Eq. (16) to numerically evaluate

$$\int_{60\ \mathrm{TeV}}^{\infty} dE f(E) A_{\mathrm{eff}}(E) \simeq 5.1\ \mathrm{m}^2. \tag{19}$$

The result of Eq. (19) now allows us to evaluate Eq. (18) analytically for cases where the initial neutrino energy is above $\sim 10^7$ GeV:

$$N \simeq T\Gamma \frac{5.1\ \mathrm{m}^2}{4\pi R_{\oplus}^2} \simeq 10^{-14} T\Gamma, \tag{20}$$

obtaining Γ from Eqs. (7) or (9) for annihilation or decay, respectively.

To place the annihilation results [Fig. 4(a)] in context, we note that searches for gamma ray and neutrino signals from DM annihilation at the galactic center limit $\langle \sigma v \rangle$ to less than about 10^{-24} to 10^{-26} $\mathrm{cm}^3\,\mathrm{s}^{-1}$ between 10^2 and 10^5 GeV [47–49], while in our region of interest above 10^5 GeV, constraints are somewhat weaker at roughly 10^{-25} to 10^{-20} cm^3 s [13], which we show in Fig. 4(a). In Fig. 4(b) we show constraints on the DM-nucleon cross section from [46], assuming A^4 scaling (see also [50]). In Fig. 4(b), the "elbow" in the constraint is defined by the boundary between the high-cross section and low-cross section scaling behavior in the capture rates Eq. (6), i.e., it falls along a line defined by $\sigma_{\chi N}/\mathrm{cm}^2 = 6.02 \times 10^{13} (m_\chi/\mathrm{GeV})$.

There is a clear tension between limits on $\sigma_{\chi N}$ for decays or annihilations of a given mass, and sensitivity to smaller values of $\langle \sigma v \rangle$: the latter requires larger DM-nucleon cross sections $\sigma_{\chi N}$ (so DM particles are trapped in Earth more efficiently), running up against the direct-detection bounds as seen in Fig. 4(b). As seen in both Figs. 4(a) and 4(b), the increased event rate for IceCube-Gen2 should not have a significant qualitative effect on these results.

This parameter tension provides context for the interpretation of other results that constrain decay or annihilation rates. For IceCube to be sensitive to neutrinos from dark matter particles that evade the direct detection bounds, the capture and thermalization process would have to be significantly altered. The effect of any such modifications can be easily checked using our approximation Eq. (20) for a dark matter distribution localized near Earth's center. We note that these comparisons can depend somewhat on simplifying assumptions, see e.g. [51].

While previous results are not exactly comparable to ours due to different assumptions, we can make some comparisons. For example, decays of dark matter particles with lifetimes on the order of 10^{27} to 10^{28} s are considered in Ref. [23] (galactic and extragalactic dark matter) and Ref. [17] (dark matter decays in Earth). Since 10^{27} s $\sim 10^{10} t_{\mathrm{E}}$, this corresponds approximately to the dot-dashed (red) curve in Fig. 4(b), where dark matter-nucleon cross sections are well above the direct detection bound. As noted in Sec. I, Ref. [17] also assumes different dark matter distributions from the thermalized distribution we have taken, considering dark matter to be uniformly distributed within Earth, or to be proportional to the density profile of baryonic matter. Therefore, it is inherently making different assumptions about dark matter properties involved in capture and thermalization.

V. SUMMARY AND CONCLUSIONS

In this paper, we have shown how rates of high-energy tau neutrinos from decaying or annihilating dark matter are related to dark matter properties such as the dark matter-nucleon cross section and decay rate or thermally averaged annihilation cross section. Given existing constraints on dark matter properties, we find that this scenario does not allow room for high-energy Earth-emerging tau neutrino events at IceCube to be interpreted in terms of decaying or annihilating dark matter. While previous work has cast doubt on such an interpretation of the anomalous ANITA events [11,28], we examine a much broader range of dark matter masses. Our explicit connection between dark matter properties—constrained experimentally—and expected IceCube event rates adds perspective to the existing literature on searches for neutrino signatures of dark matter.

Our work included a numerical simulation that showed how significant tau lepton energy losses during tau neutrino regeneration drive a wide range of initial neutrino energies toward a distinct spectrum, as shown in Eq. (16) and Fig. 2(b). When combined with estimates of dark matter capture and thermalization in relation to decay or annihilation rates, this allows for a semianalytic estimate of the IceCube HESE event rate, Eq. (20). This result provides a useful way to quickly check the effect of, for example, quite different assumptions about the dark matter capture and thermalization process.

More sensitive dedicated searches for localized ultrahigh energy tau neutrinos could be performed directly from future experiments and upgrades [44,52,53]. While these could lead to more sensitivity than we have inferred from the public IceCube HESE sample, we do not expect this to change the qualitative picture we have presented. We have also assumed that tau neutrinos are immediate decay products of the dark matter particle. If there is instead a mediator that eventually decays to neutrinos, with a lifetime allowing many mediator particles to escape Earth before decaying, IceCube could still constrain this but with reduced sensitivity that would depend on model assumptions. There are a number of other ways in which Standard Model uncertainties, dark matter model dependence, and

detector subtleties enter the above calculation. While these do not change the general features of our conclusions, future analyses or unexpected results in high-energy neutrino physics (e.g. the tau neutrino cross section [54]) could be cause to revisit this.

ACKNOWLEDGMENTS

M. S. was supported by a summer research fellowship at Bowdoin College. This research made use of the Bowdoin Computing Grid, and we thank Dj Merrill for assistance. We also thank the referees for valuable comments.

[1] K. Freese, Can scalar neutrinos or massive dirac neutrinos be the missing mass?, Phys. Lett. **167B**, 295 (1986).
[2] L. M. Krauss, M. Srednicki, and F. Wilczek, Solar system constraints and signatures for dark matter candidates, Phys. Rev. D **33**, 2079 (1986).
[3] K. Griest and D. Seckel, Cosmic asymmetry, neutrinos and the sun, Nucl. Phys. **B283**, 681 (1987); **B296**, 1034(E) (1988).
[4] A. Gould, Resonant enhancements in WIMP capture by the Earth, Astrophys. J. **321**, 571 (1987).
[5] A. Gould, Cosmological density of WIMPs from solar and terrestrial annihilations, Astrophys. J. **388**, 338 (1992).
[6] A. E. Faraggi, K. A. Olive, and M. Pospelov, Probing the desert with ultraenergetic neutrinos from the sun, Astropart. Phys. **13**, 31 (2000).
[7] I. F. M. Albuquerque, L. Hui, and E. W. Kolb, High-energy neutrinos from superheavy dark matter annihilation, Phys. Rev. D **64**, 083504 (2001).
[8] I. F. M. Albuquerque, J. Lamoureux, and G. F. Smoot, Neutrino telescopes' sensitivity to dark matter, Phys. Rev. D **66**, 125006 (2002).
[9] T. Bruch, A. H. G. Peter, J. Read, L. Baudis, and G. Lake, Dark matter disc enhanced neutrino fluxes from the Sun and Earth, Phys. Lett. B **674**, 250 (2009).
[10] A. Bhattacharya, A. Esmaili, S. Palomares-Ruiz, and I. Sarcevic, Update on decaying and annihilating heavy dark matter with the 6-year IceCube HESE data, J. Cosmol. Astropart. Phys. 05 (2019) 051.
[11] J. M. Cline, C. Gross, and W. Xue, Can the ANITA anomalous events be due to new physics?, Phys. Rev. D **100**, 015031 (2019).
[12] T. Mukherjee, M. Pandey, D. Majumdar, and A. Halder, Estimation of baryon asymmetry from dark matter decaying into IceCube neutrinos, Int. J. Mod. Phys. A **36**, 2150078 (2021).
[13] C. A. Argüelles, A. Diaz, A. Kheirandish, A. Olivares-Del-Campo, I. Safa, and A. C. Vincent, Dark matter annihilation to neutrinos, Rev. Mod. Phys. **93**, 035007 (2021).
[14] Y. Xu, Measurement of TeV dark particles due to decay of heavy dark matter in the earth core at IceCube, Phys. Dark Universe **32**, 100809 (2021).
[15] C. Guépin, R. Aloisio, L. A. Anchordoqui, A. Cummings, J. F. Krizmanic, A. V. Olinto, M. H. Reno, and T. M. Venters, Indirect dark matter searches at ultrahigh energy neutrino detectors, Phys. Rev. D **104**, 083002 (2021).
[16] R. Garani and S. Palomares-Ruiz, Evaporation of dark matter from celestial bodies, arXiv:2104.12757.
[17] M. H. Reno, L. A. Anchordoqui, A. Bhattacharya, A. Cummings, J. Eser, C. Guépin, J. F. Krizmanic, A. V. Olinto, T. Paul, I. Sarcevic *et al.*, Neutrino constraints on long-lived heavy dark sector particle decays in the Earth, Phys. Rev. D **105**, 055013 (2022).
[18] L. A. Anchordoqui, V. Barger, D. Marfatia, M. H. Reno, and T. J. Weiler, Oscillations of sterile neutrinos from dark matter decay eliminates the IceCube-Fermi tension, Phys. Rev. D **103**, 075022 (2021).
[19] S. Desai *et al.* (Super-Kamiokande Collaboration), Search for dark matter WIMPs using upward through-going muons in Super-Kamiokande, Phys. Rev. D **70**, 083523 (2004); **70**, 109901(E) (2004).
[20] A. Achterberg *et al.* (AMANDA Collaboration), Limits on the muon flux from neutralino annihilations at the center of the Earth with AMANDA, Astropart. Phys. **26**, 129 (2006).
[21] M. G. Aartsen *et al.* (IceCube Collaboration), First search for dark matter annihilations in the Earth with the IceCube Detector, Eur. Phys. J. C **77**, 82 (2017).
[22] K. Murase and J. F. Beacom, Constraining very heavy dark matter using diffuse backgrounds of neutrinos and cascaded gamma rays, J. Cosmol. Astropart. Phys. 10 (2012) 043.
[23] A. Esmaili and P. D. Serpico, Are IceCube neutrinos unveiling PeV-scale decaying dark matter?, J. Cosmol. Astropart. Phys. 11 (2013) 054.
[24] K. Murase, R. Laha, S. Ando, and M. Ahlers, Testing the Dark Matter Scenario for PeV Neutrinos Observed in IceCube, Phys. Rev. Lett. **115**, 071301 (2015).
[25] L. A. Anchordoqui, V. Barger, J. G. Learned, D. Marfatia, and T. J. Weiler, Upgoing ANITA events as evidence of the *CPT* symmetric universe, Lett. High Energy Phys. **1**, 13 (2018).
[26] L. Heurtier, Y. Mambrini, and M. Pierre, Dark matter interpretation of the ANITA anomalous events, Phys. Rev. D **99**, 095014 (2019).
[27] M. G. Aartsen *et al.* (IceCube Collaboration), Search for neutrinos from decaying dark matter with IceCube, Eur. Phys. J. C **78**, 831 (2018).
[28] I. Safa, A. Pizzuto, C. A. Argüelles, F. Halzen, R. Hussain, A. Kheirandish, and J. Vandenbroucke, Observing EeV neutrinos through Earth: GZK and the anomalous ANITA events, J. Cosmol. Astropart. Phys. 01 (2020) 012.
[29] L. Covi, M. Grefe, A. Ibarra, and D. Tran, Unstable Gravitino Dark Matter and Neutrino Flux, J. Cosmol. Astropart. Phys. 01 (2009) 029.
[30] L. Boyle, K. Finn, and N. Turok, *CPT*-Symmetric Universe, Phys. Rev. Lett. **121**, 251301 (2018).

[31] F. Halzen and D. Saltzberg, Tau-Neutrino Appearance with a 1000 Megaparsec Baseline, Phys. Rev. Lett. **81**, 4305 (1998).
[32] F. Becattini and S. Bottai, Extreme energy neutrino(tau) propagation through the Earth, Astropart. Phys. **15**, 323 (2001).
[33] J. F. Beacom, P. Crotty, and E. W. Kolb, Enhanced signal of astrophysical tau neutrinos propagating through Earth, Phys. Rev. D **66**, 021302 (2002).
[34] M. C. Gonzalez-Garcia, F. Halzen, and M. Maltoni, Physics reach of high-energy and high-statistics icecube atmospheric neutrino data, Phys. Rev. D **71**, 093010 (2005).
[35] M. H. Reno, J. F. Krizmanic, and T. M. Venters, Cosmic tau neutrino detection via Cherenkov signals from air showers from Earth-emerging taus, Phys. Rev. D **100**, 063010 (2019).
[36] A. Kochocki, V. Takhistov, A. Kusenko, and N. Whitehorn, Contribution of secondary neutrinos from line-of-sight cosmic ray interactions to the IceCube diffuse astrophysical flux, Astrophys. J. **914**, 91 (2021).
[37] J. Alvarez-Muñiz, W. R. Carvalho, A. L. Cummings, K. Payet, A. Romero-Wolf, H. Schoorlemmer, and E. Zas, Comprehensive approach to tau-lepton production by high-energy tau neutrinos propagating through the Earth, Phys. Rev. D **97**, 023021 (2018); **99**, 069902(E) (2019).
[38] J. F. Acevedo, J. Bramante, A. Goodman, J. Kopp, and T. Opferkuch, Dark matter, destroyer of worlds: Neutrino, thermal, and existential signatures from black holes in the Sun and Earth, J. Cosmol. Astropart. Phys. 04 (2021) 026.
[39] K. Griest and M. Kamionkowski, Unitarity Limits on the Mass and Radius of Dark Matter Particles, Phys. Rev. Lett. **64**, 615 (1990).
[40] H. Abramowicz and A. Levy, The ALLM parameterization of $\sigma(\mathrm{tot})(\gamma * p)$: An update, arXiv:hep-ph/9712415.
[41] A. Dziewonski, Earth structure and global, *Encyclopedia of Solid Earth Geophysics*, edited by D. E. James (Van Nostrand Reinhold, New York, 1989), p. 331.
[42] R. Abbasi *et al.* (IceCube Collaboration), The IceCube high-energy starting event sample: Description and flux characterization with 7.5 years of data, Phys. Rev. D **104**, 022002 (2021).
[43] R. Abbasi *et al.* (IceCube Collaboration), Measurement of astrophysical tau neutrinos in IceCube's high-energy starting events, arXiv:2011.03561.
[44] M. G. Aartsen *et al.* (IceCube-Gen2 Collaboration), IceCube-Gen2: The window to the extreme Universe, J. Phys. G **48**, 060501 (2021).
[45] M. G. Aartsen *et al.* (IceCube Collaboration), Evidence for high-energy extraterrestrial neutrinos at the IceCube detector, Science **342**, 1242856 (2013).
[46] M. Clark, A. Depoian, B. Elshimy, A. Kopec, R. F. Lang, and J. Qin, Direct detection limits on heavy dark matter, Phys. Rev. D **102**, 123026 (2020).
[47] A. Albert *et al.* (ANTARES Collaboration), Search for dark matter towards the Galactic Centre with 11 years of ANTARES data, Phys. Lett. B **805**, 135439 (2020).
[48] M. Ackermann *et al.* (Fermi-LAT Collaboration), Limits on dark matter annihilation signals from the Fermi LAT 4-year measurement of the isotropic gamma-ray background, J. Cosmol. Astropart. Phys. 09 (2015) 008.
[49] M. N. Mazziotta *et al.* (Fermi-LAT Collaboration), Search for dark matter signatures in the cosmic-ray electron and positron spectrum measured by the Fermi Large Area Telescope, Proc. Sci., ICRC2019 (**2020**) 531.
[50] B. J. Kavanagh, Earth scattering of superheavy dark matter: Updated constraints from detectors old and new, Phys. Rev. D **97**, 123013 (2018).
[51] M. C. Digman, C. V. Cappiello, J. F. Beacom, C. M. Hirata, and A. H. G. Peter, Not as big as a barn: Upper bounds on dark matter-nucleus cross sections, Phys. Rev. D **100**, 063013 (2019).
[52] A. V. Olinto *et al.* (POEMMA Collaboration), The POEMMA (Probe of Extreme Multi-Messenger Astrophysics) observatory, J. Cosmol. Astropart. Phys. 06 (2021) 007.
[53] A. Ishihara (IceCube Collaboration), The IceCube upgrade—design and science goals, Proc. Sci., ICRC2019 (**2021**) 1031 [arXiv:1908.09441].
[54] P. B. Denton and Y. Kini, Ultra-high-energy tau neutrino cross sections with GRAND and POEMMA, Phys. Rev. D **102**, 123019 (2020).